EWA LUBERA, KAZIMIERZ KRZEMIEŃ, PAWEŁ KRZAKLEWSKI

FROST WEATHERING OF SELECTED TATRA ROCKS
IN THE LIGHT OF LABORATORY TESTS

Abstract: Frost weathering is one of the types of physical weathering. The goal of this study was to find out how the rates and ways of frost weathering vary, based on laboratory research studies. A variety of types of Tatra rocks, their mineral composition, degree of fissuring, various capabilities of absorption of water, and porosity, all determine the progress of the process of weathering as well as its dissimilar effects and products. Generally, the breaking apart and gradual disintegration of rock into smaller fragments are the results of weathering. Rock samples, intended to be studied in the laboratory, represented rock formations of different age and various geologic units of the Western Tatra Mountains. The laboratory research studies that were conducted simulated processes occurring under natural conditions, which allowed performing an analysis of the physical properties of rocks. The rocks of the greatest and the smallest resistance to frost weathering were identified based on a calculated frost weathering index. The significant resistance of the studied Tatra rocks is influenced by their low open porosity, low capability of absorption of water, rock toughness, high degree of sorting of rock grains (grain sizes are similar), low degree of fracturing of samples in their initial state, and the presence of cementing material filling in rock pores almost entirely. The influence of texture on the disintegration of rocks was not observed, whereas the presence of mineral veins in rocks determined the way they fell apart, which occurred in samples of fine-grained conglomerate.

Keywords: frost weathering, laboratory simulation, Western Tatras

INTRODUCTION

The frost weathering is a commonly occurring process. Different environmental conditions determine different ways the process progresses and dissimilar effects and products of weathering (Hallet 1991; Hall 1992; Migoń 2006; Paasche et al. 2006). Frost weathering, leads to changes in physical properties of rocks without changing their mineral and chemical composition. Breaking apart and gradual disintegration of a rock into smaller fragments, from large rock blocks down to specks of dust. A visible indication of physical weathering is the opening up of existing discontinuities, that is fracture planes, bedding

planes (surfaces of contact between rock beds), surfaces of contact between minerals, and the creation of new ones (Migoń 2006). The primary causes of mechanical weathering include rock temperature and moisture changes, changes in stress states in rocks and the growth of foreign crystals in fissures and pores of rocks (Turkington, Paradise 2005; Migoń 2006). The role of extreme events, for example strong winds and deforestation resulting from that (Migoń et al. 2013) may also play a role in (frost) weathering.

K. Hall (1999, 2010) indicated that the fatigue of rock material due to temperature changes, which causes the expanding or shrinking of rocks, is the cause of rock disintegration. The cooled surface parts of a rock experience tension, while simultaneously the interior of the rock undergoes compression, whereas an inverse process occurs when a rock is heated. During cooling the drop in temperature inside a rock is occurring slower than on its surface, which results in the temperature inside being higher than the temperature on the surface. However, during heating the temperature on the surface of a rock increases faster than the temperature inside the rock, that is why the surface of the rock is warmer than its interior. The differences in temperature of different parts of a rock create stresses within it.

N. Matsuoka (2001, 2008) indicated that the processes that lead to the disintegration of a rock sample may progress in different ways depending on the moistening system implemented. The pore water stored in rocks is supercooled as the temperature drops below 0°C, in a closed moistening system. When the temperature of freezing is reached, supercooling stops and the temperature of pore water suddenly increases until it reaches a stable equilibrium at the freezing point, which is the result of releasing latent heat during ice formation. In an open system, the freezing of pore water usually starts at the freezing point without supercooling and it is initiated by external "ice nuclei." Expansion of rock pores starts at a temperature that is just below the freezing point, which is caused by an increasing volume of ice in the pores. The cooling of a rock down to a temperature that is below the freezing point is a necessary condition for weathering process.

Physical weathering changes the properties of the material being transported, and the "mechanical" composition of frost weathering products determines how they will be transported on hillslopes, and thus it determines the method of altering the relief of the slopes (Tricart 1960). Frost weathering is an especially significant process in periglacial areas, and its rate depends most of all on the type of rocks and their petrographic and mineralogic characteristics (André 1996; Paasche et al. 2006; Gądek et al. 2016).

The susceptibility of rocks to frost weathering depends primarily on: i/climate conditions – most of all on the variability of air temperature and

humidity, ii/ properties of rocks – mineral composition, the degree to which the minerals are bound together, iii/ texture, cementing material, porosity, fracture system, rock strength, iv/ orographic conditions and geographic orientation (affecting exposure to sunlight), v/ duration of geomorphological processes (Traczyk, Migoń 2000; Migoń 2006).

The mechanism of frost weathering has been a subject of discussion for many years. There are several theories explaining how frost weathering causes rock disintegration (Bland, Rolls 1998):

a. The freezing of water, present in fractures, starts at the surface and runs from the opening of the fissure deeper inside. Ice forms a plug at the surface, and a closed system is created, in which the volume of water increases as it turns into ice. The increasing volume causes an increase in pressure. The high pressure leads to the disintegration of rock. The necessary condition for creating sufficiently high pressure is that the rate of freezing must be over $0.1°C·min^{-1}$ and significantly negative temperatures must be reached.

b. Migration of water towards ice cells that are forming, as a result of differences in thermodynamic potential, leads to the creation of high pressure and the disintegration of a rock. The reaching of a temperature that is in the range from -5°C to -15°C and the rate of freezing that is in the range from less than 0.1 to 0.5°C per hour, at which the fastest development of fissures is noted, is a necessary precondition to initiate the process.

c. Single molecules of water, contained in fissures or rock pores, become oriented with respect to a charged surface of minerals, in such a way that one end binds with the mineral surface, and the second moves away. In negative temperatures that are close to zero, molecules may not freeze up and may not become reoriented. Electrostatic repulsion occurs in narrow fissures and pores having a small diameter, when similarly charged free poles of molecules get near each other, located on the opposite walls of the fissure. Electrostatic repulsion increases as temperature decreases and leads to the damaging of a rock.

d. The freezing of a rock surface, which came in contact with water earlier, forms a barrier for water migration. Subsequently, the water contained in rock pores close to the surface, freezes, and the molecules that have increased in volume, push out the remaining unfrozen water deeper into the rock. In the case of rocks, which are sufficiently resistant to friction created by moving water molecules, the rock may disintegrate. This occurs due to the high hydraulic pressure that is created (Bland, Rolls 1998).

The aim of the research was to learn the rate and method of frost weathering of Tatra rocks based on laboratory tests.

STUDY AREA
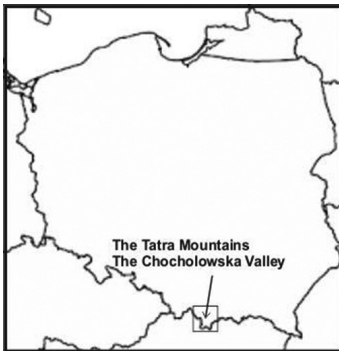
Fig.1. Location of the study area – the Western Tatra Mountains (Poland)

Rock samples, intended to be studied in the laboratory, were collected in the Chochołowska Valley, the westernmost and largest of the valleys in the Polish part of the Western Tatras (Fig. 1). Its area is 35.6 km^2, and its length is 9.7 km. This area is characterized by a high mountain landscape with well-developed post-glacial relief features and by a presence of altitudinal zones of vegetation and climate so typical of Central European mountains.

The upper part of the valley is built of formations of the crystalline series of the Western Tatras (rock sample collection sites 3, 4, 5; Fig. 2), whereas the lower part of the valley is composed of formations of the High Tatra carbonate series (sampling sites 2, 6, 7; Fig. 2) and of the lower montane series (sampling site 1) (Piotrowska et al. 2015). The rock sampling sites are mainly located at high elevations, in the upper tree line zone and above it.

The Chochołowska Valley lie in the high-mountain climate of the temperate zone. According M. Hess (1965) the zero isotherm (0°C) of the mean annual air temperature occurs at an altitude of 1,800 m a.s.l., but at present is over 100 m higher (Łupikasza, Szypuła 2019). There are significant annual and daily air temperature fluctuations. The difference between the daily maximum and daily minimum temperature can exceed 20°C. The number of days on when the air temperature falls below 0°C is linked to the mean monthly temperature (Hess 1965). The mean annual precipitation amount in the lower part of the Chochołowska Valley is less than 1,200 mm; in its middle part it is in the interval from 1,200 to 1,600 mm, and on the surrounding peaks the precipitation amounts are more than 1,600 to 1,800 mm (Łupikasza, Szypuła 2019).

The study sites, where the amount of material falling of the rock walls was measured, were located in the lower montane zone (sites 2, 6, 7), in the upper montane zone (site 1), and in the subalpine zone (sites 3, 4, 5) (Fig. 2). Rock samples for laboratory tests were collected at 7 locations – the Mnichy Chochołowskie (site 1), the Grześ Mt. (site 2) and the Wołowiec Mt. (sites 3, 4; 2 samples), the Dudowe Turnie (site 5), the Kominiarski Wierch (site 6), and in the Dudowa Valley (site 7), (Fig. 2). The testing for resistance to frost weathering was performed for 7 types of rocks – dolomite breccia, organodetrital limestone, fine-grained conglomerate, quartzite sandstone, white granite, brown granite and amphibolite (Table 1).
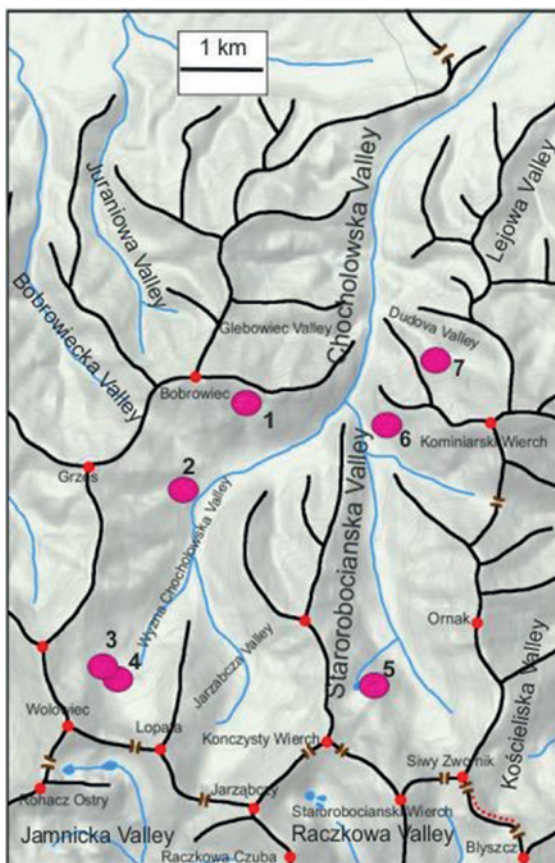
Fig. 2. Location of rock samples: 1 – dolomite breccia, 2 – quartzite sandstone, 3 – white granite, 4 – amphibolite, 5 – brown granite, 6 – fine-grained conglomerate, 7 – organodetrital limestone (author's own work)

Table 1.

Rock collection sites and rock types selected for testing for their resistance to frost weathering

Sample no.	Location	Altitude (m a.s l.)	Lithology
1	Mnichy Chochołowskie	1,465	dolomite breccia
2	Grześ Mt.	1,175	quartzite sandstone
3	Wołowiec Mt.	1,635	white granite
4	Wołowiec Mt.	1,630	amphibolite
5	Dudowe Turnie	1,645	brown granite
6	Kominiarski Wierch	1,115	fine-grained conglomerate
7	Dudowa Valley	1,125	organodetrital limestone

RESEARCH METHODS

The study included laboratory analyses of the physical properties of selected Tatra rocks and a simulation of frost weathering under laboratory conditions.

COLLECTION OF ROCK SAMPLES

For each type of rock, 5–6 cylindrical cores were cut out of rock blocks brought from rock collection sites. The height and diameter of the base of each core were 5 cm each. The samples were marked, for example, 1/1, 2/2. 4/1. Smaller cylinders (2.5 cm in height and 5 cm in diameter) were cut of from one core for each type of rock. Smaller cylinders were intended for testing for compressive strength and tensile strength. The remaining portion of the material was used to determine open porosity, bulk density as well as to perform a petrographic analysis and an X-Ray Diffraction (XRD) analysis of the investigated rocks (Figs. 3, 4).

Fig. 3. Block and cut-out rock samples, for simulation of weathering and strength tests, on the example of sample no. 4. a) rock sample before core cutting, b) rock sample after core cutting
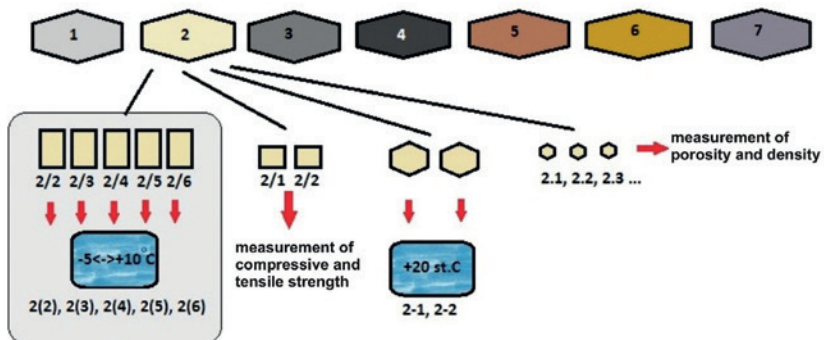
Fig. 4. Procedure for carrying out laboratory tests, on the example of sample no. 2. Numbers 1-7 in the top row refer to the sample sets from individual study sites

INVESTIGATION OF SELECTED PETROPHYSICAL PROPERTIES OF ROCKS

In order to determine the mineral composition of the studied rock samples, appropriate cutting and grinding tasks were performed at the machining laboratory of the College of Geology, Geophysics and Environmental Protection of the AGH University of Science and Technology. Subsequently, a microscopic analysis of the rock samples was performed. The analysis was performed at the Institute of Geology of Jagiellonian University in Krakow. The purpose of these analyses was to determine texture, rock structure, type of cementing material and porosity, and the degree of filling in of pore spaces in the studied rocks.

X-Ray Diffraction (XRD) was performed for each rock sample using a Philips X'Pert APD diffractometer at the Institute of Geological Sciences of Jagiellonian University. Strength tests were performed at the Institute of Orogenic Belt Mechanics of the Polish Academy of Sciences. Compressive strength and tensile strength were measured. The porosity of the rock samples was determined using the water saturation method (Chen et al. (2004). The measurements were performed at the Department of Hydrogeology and Engineering Geology of the AGH University of Science and Technology. Bulk density was determined as a ratio of the mass of the sample to its total volume, and it depends on the proper density of the granular skeletal material and on the porosity of the rock. The bulk density tests were performed at the laboratory of the College of Geology, Geophysics and Environmental Protection of the AGH University of Science and Technology.

FROST WEATHERING SIMULATION

A simulation of frost weathering was conducted at the Low Temperature Laboratory at the Institute of Geography and Spatial Management of Jagiellonian University. The equipment used here included a refrigeration unit, model CI/1400/LT/2D, driven by a temperature controller of the STE 3 type, made by JBG-2. Two freeze-thaw cycles, within the temperature range from -5° to +10°C, took place within each 24-hour period. The boundary temperatures were maintained for 5 hours. The rock samples, immersed up to a height of about 2 cm in distilled water, were placed in plastic containers. The containers were kept closed during the simulation in order to limit moisture changes.

Observations of the condition of samples and measurements of the weathered material were performed while the simulation was still in progress. In order to detect changes in the immersed samples, certain measurements

were repeated, initially every 20 freeze-thaw cycles, and later roughly every 100 cycles, which included the measurement of the mass of a sample that was air-dry (m) and saturated with water (m_w), capability of samples to absorb water (A_b), an ultrasonic test, and the measurement of the attenuation coefficient (A). The measurements were performed at the Institute of Orogenic Belt Mechanics of the Polish Academy of Sciences in Krakow. An ultrasonic test entails the measurement of the velocity of a longitudinal acoustic wave transmitted through a rock sample (V_p, Nowakowski et al. 2003). The sample being tested is placed between two steel heads, which are equipped with an emitter and a receiver of a longitudinal acoustic wave. During the test, the time it takes for the wave to pass through a sample is measured. The value of the velocity of a longitudinal wave (V_p) is obtained by dividing the height h of the sample by the real time (t_p), which is the difference of the time measured (t_z) and the start time (t_0).

The intensity of an ultrasonic ray (wave) reaching the receiver is significantly lower than the intensity of an ultrasonic ray (wave) emitted by the emitter. Wave refraction is related to the lack of uniformity of the tested material. Structural discontinuities such as cracks, grain boundaries, indentations, and pores cause a change in the direction of small portions of ultrasound energy from the main ray (Baranowska, Garbiak 1999). A decrease in wave intensity is expressed by the attenuation coefficient (A). The acoustic properties of rocks are largely determined by the properties of minerals they are composed of; high velocities are typical of rock-building minerals (Chrzan 1994).

A sample was dried at a temperature of 75°C for 48 h and weighed in an air-dry state before every subsequent ultrasound test. After an ultrasound test, the samples were placed in a vacuum in order to remove air out of rock pores (until the mass is stabilized) and saturated with water again. Then, the measurement of the mass of a sample saturated with water (m_w) was performed in order to control the capability of samples to absorb water (A_b).

The frost weathering index may be calculated based on the obtained values of V_p (Matsuoka 1990) and allows to compare the resistance of selected rocks to the investigated process. The lower the value of the index R_f, the higher the resistance of a given rock to the effects of freezing.

$$R_f = (V_{p0} - V_{pk})/V_{p0} \cdot k \text{ cycles}^{-1}$$

where:
V_{p0} – velocity of longitudinal ultrasonic wave before the start of freeze-thaw cycles (km·s^{-1})
V_{pk} – velocity of longitudinal ultrasonic wave after k cycles (km·s^{-1})
k – number of freeze-thaw cycles

STUDIES OF FROST WEATHERING PRODUCTS

The weathering simulation was concluded after 900 freeze-thaw cycles. The rock fragments were dried over a 24-hour period at a temperature of 105°C. Grain size analysis of the obtained weathered rock products was performed using a FRITSCH Analysette 3 PRO Vibratory Sieve Shaker, in order to determine the variation of the grain size of the rock fragments. The vibration amplitude was set to 0.5 mm, and the vibration time to 10 minutes. The mass and percentage share of gravel, sand, silt and clay fractions were determined. The measurements of mass were performed with the accuracy of up to 0.01 g.

RESEARCH RESULTS

SELECTED PHYSICAL PROPERTIES OF THE STUDIED ROCKS

Laboratory study of the rocks has shown that sample 1 (dolomite breccia) is characterized by an average open porosity of 3.87%, sample 2 (quartzite sandstone) 0.69%, 3 (white granite) 1.50%, 4 (amphibolite) 0.36%, 5 (brown granite) 1.90%, 6 (conglomerate) 2.59% and 7 (limestone) 1.17%. All the studied rocks may be assessed to belong to a category of rocks of low open porosity, which is less than 5%.

The study of bulk density produced the following results: dolomite breccia (1) – the average density was 2.69 $Mg·m^{-3}$; quartzite sandstone (2) – 2.64 $Mg·m^{-3}$; white granite (3) – 2.60 $Mg·m^{-3}$; amphibolite (4) – 2.87 $Mg·m^{-3}$; brown granite (5) – 2.58 $Mg·m^{-3}$; fine-grained conglomerate (6) – 2.56; organodetrital limestone (7) – 2.68 $Mg·m^{-3}$.

As the structure of samples became damaged, their capability to absorb water increased. In the case of the investigated Western Tatra rocks, changes in the capability to absorb water were very small while the frost weathering simulation was still in progress. Rocks characterized by the lowest capability to absorb water included amphibolite, while the greatest capability to absorb water was typical of dolomite.

The greatest increase in the capability of the studied rocks to absorb water, while the laboratory experiment was still in progress, was measured for the dolomite samples; the increase was about 0.3%. The capability of the dolomite samples to absorb water increased from an initial value of 0.94–2.28% to 1.14–2.45%, after more than 700 freeze-thaw cycles (Fig. 5).

In amphibolite and conglomerate samples, the increase in the capability to absorb water was 0.1–0.2%. In amphibolite, it changed from its initial value of 0.05–0.09% to 0.09–0.15%, after more than 700 freeze-thaw cycles.
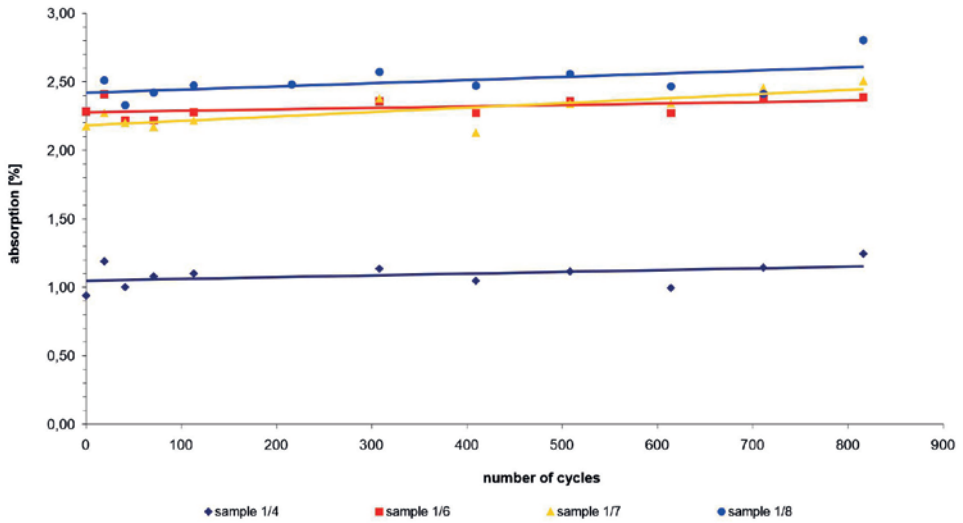
Fig. 5. Capability to absorb water for dolomite samples in a simulation of frost weathering (linear pattern illustrates only tendencies of change)

The capability to absorb water in conglomerate increased from 0.27–0.78% to 0.29–0.82% after about 700 freeze-thaw cycles had taken place.

In sandstone, granite and limestone an increase in the capability to absorb water was about 0.1%. The capability to absorb water in sandstone samples increased from its initial value of 0.19–1.25% to 0.24–0.32%, after almost 800 freeze-thaw cycles. In granite samples the capability to absorb water increased from 0.43–0.82% to 0.49–0.92% after almost 800 freeze-thaw cycles had taken place. The discussed parameter changed only slightly in organodetrital limestone.

The performed strength tests supplied the following information – carbonate rocks (dolomite breccia and organodetrital limestone) are characterized by average strength, amphibolite is characterized by high strength, and the remaining rock types by very high strength. An exceptionally high strength is typical for quartzite sandstone, sample number 2 – 405.3 MPa and fine-grained conglomerate, sample 6 (Table 2).

Table 2.

Compressive strength (Rc) and tensile strength (Rr) of the studied Tatra rocks

Sample no.	1	2	3	4	5	6	7
Rc [MPa]	77.6	405.3	284.2	167.2	217.1	368.2	77.4
Rr [MPa]	7.2	7.4	6.4	13.6	6.8	18.1	5.2

PROGRESS OF THE SIMULATED FROST WEATHERING
OF SELECTED ROCKS – MACROSCOPIC CHANGES

Disintegration of rock samples during the laboratory experiment most often occurred when rock fragments were falling of the sides and edges of rock samples, of surfaces that had already been damaged earlier. What was occurring was that single grains were breaking away from rock fissures, which resulted in the widening of cracks (Table 3).

The quickest disintegration occurred in dolomite samples, and it occurred since the beginning of the laboratory simulation. Rock fragments of different dimensions, from less than 1 mm to almost 2 cm in diameter, broke of. The splitting up of fragments that previously had fallen of a rock sample was observed. The rock fragments were irregular in shape and sharp-edged. The greatest and most frequent changes occurred in sample 1/7 (Fig. 6.).
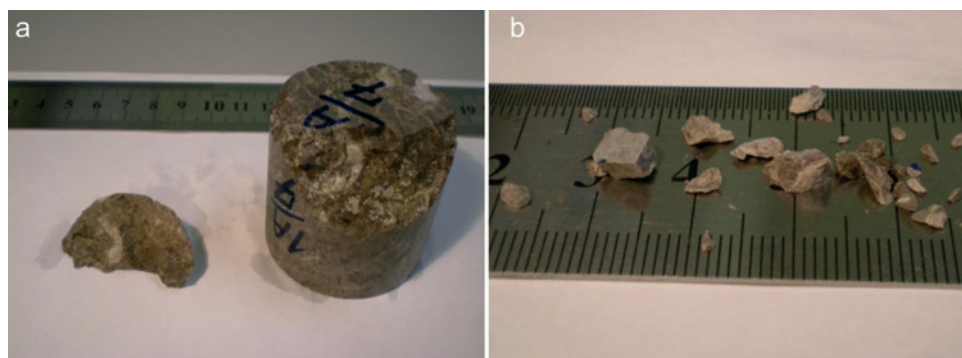
Fig. 6. Condition of sample 1/7 (dolomite breccia) after 149 freeze-thaw cycles. a) rock before cycles, b) rock after 149 cycles

Single grains of quartz, with a diameter of less than 0.5 mm, were the only bits that fell of the quartzite sandstone samples. Macroscopic changes were also not observed in amphibolite samples, sample 4/3 was an exception, because fragments with a 1.0–1.5 mm diameter had broken of that sample (Table 3).

The disintegration of the studied varieties of Tatra granite occurred in a different manner, depending on type of granite. Brown granite rocks did not undergo significant macroscopic changes. White granite samples underwent little breakup, which occurred by the detaching and falling of the laminae of muscovite, grains of quartz and rock fragments having several millimeters in size, up to a maximum of 1 cm. Disintegration occurred in the first 100 freeze-thaw cycles and no significant changes were recorded later (Table 3).

Table 3.

Breakdown of rock samples during the simulation of frost weathering

Type of rock	Sample no.	Number of freeze-thaw cycles	Decay of the sample observed during frost weathering simulation
Dolomite breccia	1/4	13	2 rock fragments: dimensions 2.0 by 1.0 mm
		71	Fragment: dimensions 1.2 by 1.0 by 0.3 cm, broken of the edge of the sample
		711	Fragment: dimensions 8.0 by 4.0 by 2.0 mm; 7.0 by 5.0 by 3.0 mm
	1/6	13	Fragment: dimensions 4.0 by 6.0 mm
		308	Fragment: dimensions 7.0 by 6.0 by 2.0 mm broken of the edge of the sample
	1/7	41	5 fragments of sizes from 2.5 mm to 6.0 mm and smaller fragments of the diameter of 1.0-1.5 mm
		71	2 fragments: dimensions 2.5 by 2.0 mm; 1.0 by 1.0 mm
		149	Fragment: dimensions 4.0 by 1.7 by 1.5 cm broken of the edge of the sample and 15 fragments having dimensions from 1.0 mm to 7.0 mm and numerous smaller fragments
		409	Fragment: dimensions 6.0 by 3.0 by 2.0 mm and fragments of up to 0.5 mm in diameter
		508	Smaller fragments breaking of the fragment, which fell of a sample earlier, then the splitting up of that chip into 2 parts
		816	Fragments having dimensions from 0.2 cm to 1.4 cm and numerous fragments having dimensions of several millimeters
	1/8	308	Fragment: dimensions 5.0 by 3.0 by 3.0 mm
		816	Fragments having dimensions from 1.0 to 4.0 mm
Quartzite sandstone	2/2		
	2/3		
	2/4		Lack of products of the disintegration of rock samples
	2/5		
	2/6		
White granite	3/2	84	Fragments: dimensions 3.0 by 1.0 mm; 3.5 by 1.0 mm and smaller grains of quartz
		23	Sediment, broken of the surface of a fissure, the fissure has widened from 1.0 mm to 1.5 mm
	3/3	84	Numerous fragments of dimensions from 1.0 mm to 4.0 mm and smaller grains of quartz and laminae (sheets) of muscovite

Type of rock	Sample no.	Number of freeze-thaw cycles	Decay of the sample observed during frost weathering simulation
White granite	3/4		Lack of products of the disintegration of rock samples
	3/5		
	3/6	42	3 fragments: dimensions 9.0 by 6.0 mm; 2.0 by 1.5 mm; 2.0 by 1.5 mm
Amphibolite	4/2		Lack of products of disintegration of rock samples
	4/3	57	2 fragments: dimensions 1.5 by 1.0 mm; 1.0 by 1.0 mm
	4/4		Lack of products of the disintegration of rock samples
	4/5		
Brown granite	5/2		Lack of products of the disintegration of rock samples
	5/3		
	5/4		
	5/5		
Fine-grained conglomerate	6/4	18	Numerous fragments: dimensions max 1.0 by 1.5 mm, most fragments are smaller
		700	Fragments: dimensions 1.1 by 0.7 by 0.3 cm; 1.2 by 0.4 by 0.1 cm; 4.0 by 3.0 by 3.0 mm
	6/5	3	Sediment - grains of the diameter smaller than 0.5 mm
		18	Numerous fragments: max dimensions 1.0 by 1.5 mm, most fragments are smaller
	6/7	48	Fragment: dimensions 3.7 by 1.8 by 1.3 cm
		398	Fragments having dimensions from 1.0 mm to 6.0 mm
	6/8	805	Splitting of the sample into two parts
	6/9		Lack of products of the disintegration of rock samples
Organodetrital limestone	7/1	60	Fragment: dimensions 1.0 cm by 0.6 cm by 0.6 cm
		704	Fragments having dimensions from 0.6 mm to 5.0 mm
	7/2		Lack of products of the disintegration of rock samples
	7/5	3	Grains of a diameter up to 0.5 mm
		18	Numerous fragments: maximum dimensions 1.0 by 1.5 mm, most fragments are smaller
		38	Fragments: dimensions 3.0 by 2.0 mm; 2.0 by 0.5 mm, smaller chips of a diameter of 1.0 mm or less
		60	6 fragments having dimensions from 0.5 mm to 2.0 mm
	7/7		Lack of products of the disintegration of rock samples

The disintegration of fine-grained conglomerate was evident. It occurred by the falling out of numerous fragments of different sizes, from several mm to 2 cm. The disintegration occurred gradually during the laboratory experiment (Table 3). It was also observed that the disintegration was related to the pattern of calcite veins (Figs. 7, 8).
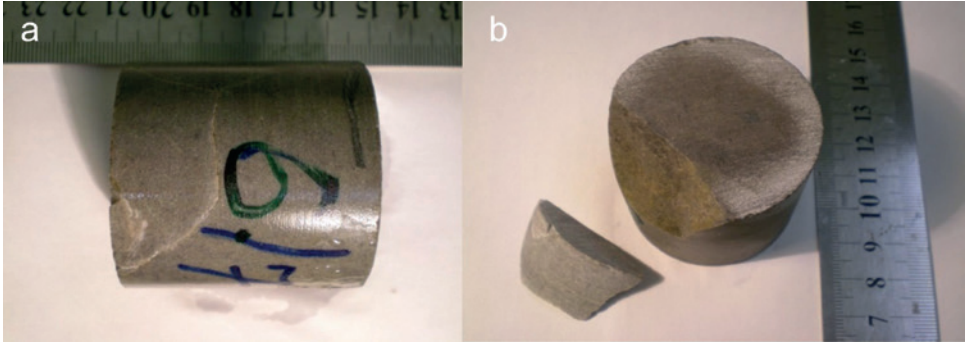
Fig. 7. Test condition of sample 6/7 – fine-grained conglomerate. a) at the beginning of the simulation, b) after 48 cycles
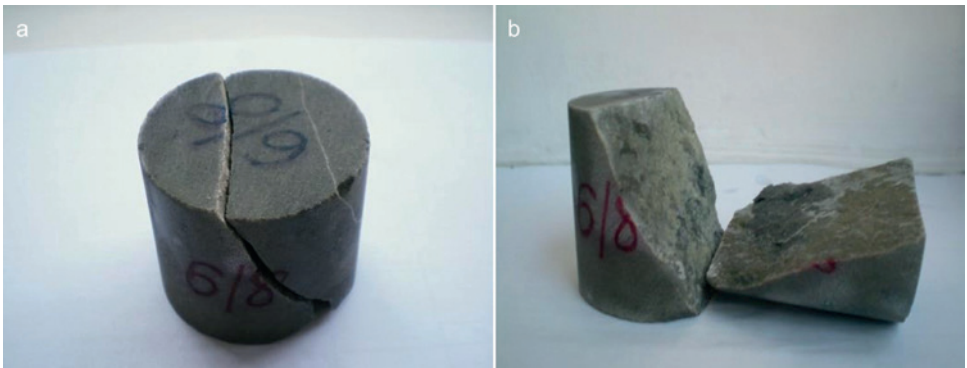
Fig. 8. Disintegration of sample 6/8 - fine-grained conglomerate, the 805th cycle. a) rock before cycles, b) rock after 149 cycles

The disintegration of organodetrital limestone occurred primarily in the first 100 freeze-thaw cycles. Numerous rock fragments, of dimensions from less than 0.5 mm to almost 1.5 cm, fell of. The rock fragments were sharp-edged and irregular in shape (Table 3).

DAMAGE TO THE STUDIED ROCKS BASED ON MEASUREMENTS OF VELOCITY OF THE ULTRASOUND WAVE

After more than 800 cycles, a clear decrease occurred in the velocity of the ultrasound wave (V_p) in dolomite samples (number 1), from its initial value of 3.97–4.40 to 2.91–3.08. The largest drop was recorded in the case of sample 1/7 (Fig. 9a). The recorded, clear decrease in the wave velocity
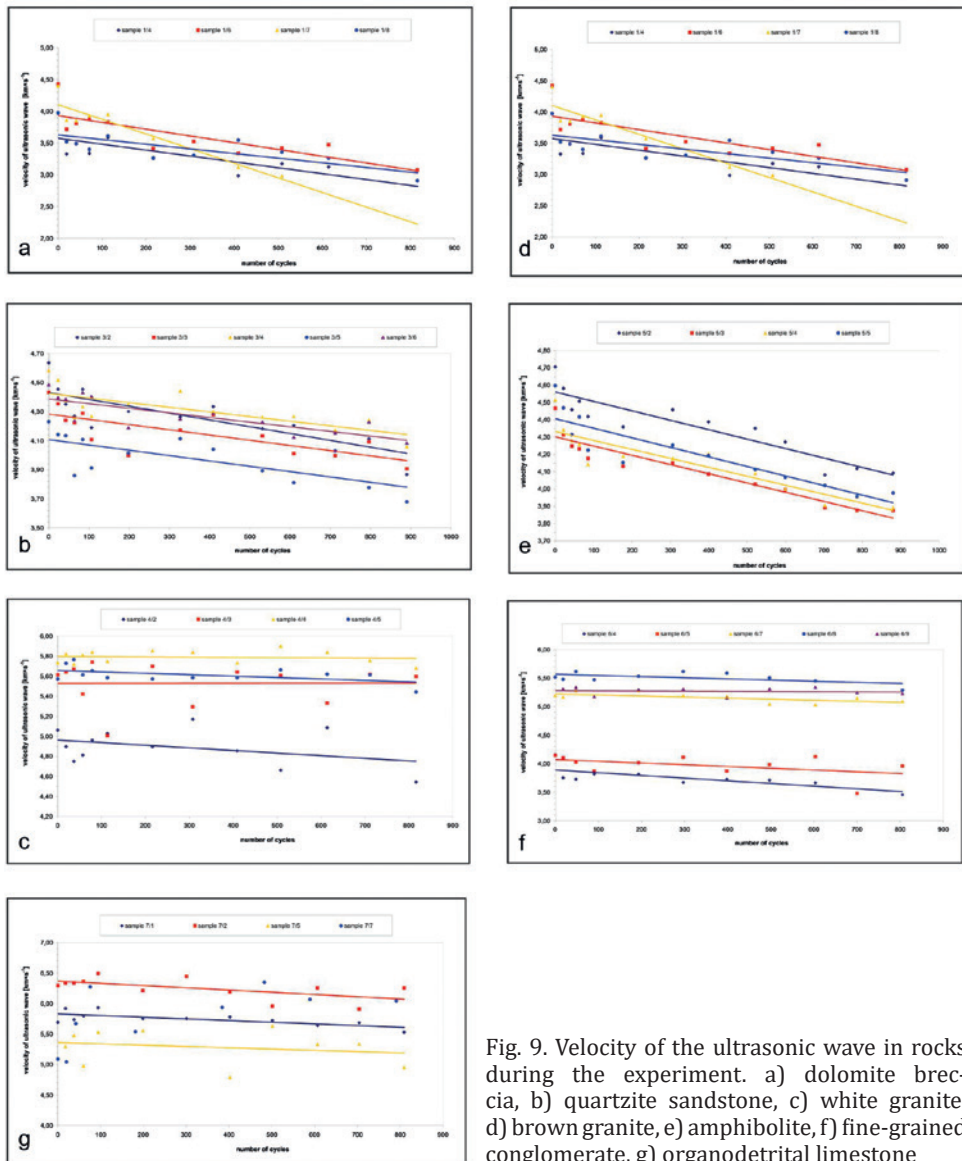
Fig. 9. Velocity of the ultrasonic wave in rocks during the experiment. a) dolomite breccia, b) quartzite sandstone, c) white granite, d) brown granite, e) amphibolite, f) fine-grained conglomerate, g) organodetrital limestone

indicates that damage to the structure of dolomite samples had occurred. The calculated frost weathering index (R_f) is $4.2 \cdot 10^{-4} \cdot cycles^{-1}$.

The decrease in the velocity of the ultrasonic wave in the studied quartzite sandstone samples (number 2) was insignificant or did not occur. The values of V_p decreased from 4.96–5.29 to 4.89–5.18 after 900 freeze-thaw cycles (Fig. 9b). The index R_f, was $0.2 \cdot 10^{-4} \cdot cycles^{-1}$ and it was the lowest for the studied rocks.

After almost 900 freeze-thaw cycles, a decrease in the velocity of the ultrasonic wave occurred in white granite samples (number 3), declining from 4.23–4.64 to 3.87–4.08. In white granite samples (number 5) a decrease in the value of the parameter V_p was recorded as it declined from 4.47–4.71 to 3.88–4.09 (Fig. 9c, 9d). The frost weathering index for both studied rocks reached similar values – $1.4 \cdot 10^{-4} \cdot cycles^{-1}$ and $1.5 \cdot 10^{-4} \cdot cycles^{-1}$ (Figs. 9c, 9d).

A barely noticeable decrease in the velocity of the ultrasonic wave occurred, from 5.06–5.73 to 4.54–5.68, in amphibolite (sample number 4) after 800 freeze-thaw cycles. The frost weathering index was low – $0.4 \cdot 10^{-4} \cdot cycles^{-1}$ (Fig. 9e).

After 800 freeze-thaw cycles, a decrease in the value of the investigated parameter V_p was recorded in fine-grained conglomerate samples (number 6) as it declined from 4.15–5.52 to 3.46–5.29. The frost weathering index was $0.7 \cdot 10^{-4} \cdot cycles^{-1}$ (Fig. 9f). The studied conglomerate samples show significant differences in the initial value of the velocity of the ultrasonic wave (Fig. 9g).

GRAIN SIZE CHARACTERISTICS OF THE WEATHERED ROCK SUBSTANCE PRODUCED

After the laboratory experiment had ended, different amounts of weathered substance were obtained from 35 samples, the initial weight of which was in the interval from about 160 to about 200 g. The mass of the weathered substance produced ranged from less than 0.01 g to 12.86 g, which in terms of a percentage share was in the range from less than 0.01 to 6.80% of the initial sample mass. The gravel fraction dominated in samples of dolomite and conglomerate and in single samples of white granite and limestone. Either the sand or silt and clay fraction dominated in the weathered product obtained from the remaining samples (Table 4).

After 816 simulated freeze-thaw cycles had been performed, it was shown that the weathered rock material obtained from dolomite sample number 1/7 had the largest mass – 12.86 g. The mass of weathered material produced from each of the remaining dolomite samples was found to be in the interval from 0.23 to 1.31 g. The percentage share of the weathered mass in the initial sample mass was in the interval from 0.12 to 6.80%. The weathered material

Table 4.

Characteristics of debris produced from rock samples as a result of simulated frost weathering

| Sample | Initial mass (g) | Gravel fraction | | Sand fraction | | Silt and clay fraction | | Total weathered mass (g) | Share of weathered material in initial sample weight (%) |
		mass (g)	share (%)	mass (g)	share (%)	mass (g)	share (%)		
1/4	192.78	0.75	83.3	0.10	11.1	0.05	5.6	0.90	0.47
1/6	186.21	0.10	43.5	0.08	34.8	0.05	21.7	0.23	0.12
1/7	189.13	11.21	87.2	1.55	12.0	0.10	0.8	12.86	6.80
1/8	187.12	0.97	74.1	0.27	20.6	0.07	5.3	1.31	0.70
2/2	189.63	0	0	< 0.01		< 0.01		< 0.01	
2/3	186.63	0	0	< 0.01		< 0.01		< 0.01	
2/4	190.48	0	0	< 0.01		< 0.01		< 0.01	
2/5	185.73	0	0	< 0.01		< 0.01		< 0.01	
2/6	186.31	0	0	< 0.01		< 0.01		< 0.01	
3/2	182.97	0	0	0.03	100.0	0	0	0.03	0.02
3/3	183.60	0	0	0.12	92.3	0.01	7.7	0.13	0.07
3/4	183.20	0	0	0.01	100.0	0	0	0.01	0.01
3/5	162.02	0	0	0.01	100.0	0	0	0.01	0.01
3/6	184.98	0.24	85.7	0.04	14.3	0	0	0.28	0.15
4/2	206.23	0	0	< 0.01		< 0.01		< 0.01	
4/3	204.16	0	0	< 0.01		< 0.01		< 0.01	
4/4	202.39	0	0	< 0.01		< 0.01		< 0.01	
4/5	207.48	0	0	< 0.01		< 0.01		< 0.01	
5/2	182.92	0	0	< 0.01		< 0.01		< 0.01	
5/3	184.11	0	0	0.04	100.0	0	0	0.04	0.02
5/4	183.86	0	0	< 0.01		< 0.01		< 0.01	
5/5	183.44	0	0	0	0	0.01	100.0	0.01	0.01
6/4	184.07	0.36	90.0	0.02	5.0	0.02	5.0	0.40	0.22
6/5	184.57	0	0	0.03	60.0	0.02	40.0	0.05	0.03
6/7	188.85	8.00	99.4	0.03	0.4	0.02	0.2	8.05	4.26
6/8	186.48	0	0	0.01	33.3	0.02	66.7	0.03	0.02
6/9	189.17	0	0	0.01	25.0	0.03	75.0	0.04	0.02
7/1	181.35	1.61	86.1	0.15	8.0	0.11	5.9	1.87	1.03
7/2	156.31	0	0	0.02	16.7	0.10	83.3	0.12	0.08
7/5	184.98	0.04	14.8	0.09	33.3	0.14	51.9	0.27	0.15
7/7	179.73	0	0	0.12	42.9	0.16	57.1	0.28	0.16

produced from the dolomite samples was mostly composed of the gravel fraction (up to 87%), whereas the percentage share of the silt and clay fraction was the smallest one (Table 4, Fig. 10).

A weathered rock substance, the mass of which did not exceed 0.01 g, was created out of portions of quartzite sandstone samples (no. 2) after 886 freeze-thaw cycles and out of amphibolite samples (no. 4) after 816 cycles (Table 4, Fig. 10).

An insignificant mass of weathered material was obtained from the Tatra granite samples after 880–890 freeze-thaw cycles, ranging from less than 0.01 to a maximum of 0.28 g. More weathered material originated from white granite than from brown granite. The percentage share of the weathered material in the initial mass of the granite rock samples ranged from 0.01 to 0.15. The largest amount of weathered material was obtained from sample no. 3/6. The sand fraction generally dominated, but the gravel fraction dominated in sample 3/6, as it was 85.7% of the mass of the weathered material (Table 4, Fig. 10).

A weathered material in the amount from 0.03 to 8.05 g was created out of parts of the fine-grained conglomerate samples after 805 freeze-thaw cycles. The largest amount of weathered material was obtained from sample no. 6/7. The percentage share of the weathered material in the initial mass of the investigated samples ranged from 0.02 to 4.26%. In the case of samples from which an insignificant mass of weathered material was generated (6/5, 6/8 and 6/9), the weathered material was either dominated by the silt and clay fraction or the share of the silt and clay fraction and the share of the sand fraction were comparable. In the case of samples from which a greater mass of weathered material was obtained (6/4, 6/7), gravel was clearly the fraction that dominated the weathered material produced (Table 4, Fig. 10).

After 809 freeze-thaw cycles, organodetrital limestone samples produced 0.12 to 1.87 g of weathered material. The largest amount of weathered material was obtained from sample no. 7/1, as the mass of the weathered material obtained was about 1% of the initial sample mass. The weathered material that originated from sample 7/1 was dominated by the gravel fraction (Table 4, Fig. 15). In the case of limestone and conglomerate, dissolution occurred along fractures and cleavage planes of the rocks. As a result of this, calcium and magnesium cations as well as chloride Cl^- and sulfate (VI) SO_4^{2-} anions precipitated.

Fig. 10. Conditions of selected rock samples: a) before weathering simulation, b) after completion of frost weathering simulation, c) picture of the result of weathering; 1 – dolomite breccia, 2 – quartzite sandstone, 3 – white granite, 4 – amphibolite, 5 – brown granite, 6 – fine-grained conglomerate, 7 – organodetrital limestone

FROST WEATHERING INDEX

Based on the calculated frost weathering index R_f (Table 5), dolomite breccia is least resistant to frost weathering. Subsequently, the studied rock types were ordered by their increasing resistance as follows: granite varieties, fine-grained conglomerate, organodetrital limestone, amphibolite. Quartzite sandstone is the rock that is the least susceptible to frost weathering.

Using the percentage share of the produced weathered material with respect to the initial mass of the investigated rock samples (Table 5) as a guide, dolomite breccia is also the least resistant one of the listed rocks. Then, the rest of the rock types could be arranged according to gradually increasing resistance. The list would be ordered as follows: fine-grained conglomerate, organodetrital limestone, varieties of granite, amphibolite. Quartzite sandstone is the least susceptible to frost weathering.

Table 5.
Rf index and share of generated weathered material for the studied types of rocks

Index	Unit	Dolomite	Quartzite sandstone	White granite	Amphi-bolite	Brown granite	Conglo-merate	Limestone
Rf	$10^{-4} \cdot \text{cycles}^{-1}$	4.2	0.2	1.4	0.4	1.5	0.7	0.4
Share of material generated by weathering	%	0.12–6.80	< 0.01	0.01–0.15	< 0.01	<0.01–0.02	0.02–4.26	0.08–1.03

DISCUSSION AND CONCLUSIONS

Difficulty in making comparisons of frost weathering research results is caused by differences in the rock types studied in the laboratory and by their physical properties. Conditions, under which experiments are performed by different researchers, differ significantly. Different temperature ranges, different duration of freeze-thaw cycles, and different moisture conditions are used. Various indicators are used to assess the resistance of rocks to frost weathering, which makes resistance comparisons difficult. It may be stated based on

the research results obtained by A. Martini (1967) and on the results presented in this paper that the influence of chemical weathering is seems to be significant in the case of carbonate rocks. Chemical weathering intensifies the processes of physical weathering by way of creating or enlarging voids in rock, which are accessible to water or salt crystals. In the case of rocks studied in the present study, the process of dissolution affected dolomite and conglomerate rocks the most, and to a lesser degree also amphibolite and limestone rocks.

A. Martini (1967) notes that mono-mineral, fine-crystalline, massive rocks are more resistant to frost weathering action. The disintegration of these type of rocks is related to discontinuities existing within their structure. Mono-mineral quartzite sandstone exhibited the highest resistance among the studied Western Tatra rocks. M. F. André (1996) also emphasized that rocks, the mineral composition of which is dominated by quartz, belong to the most resistant to frost weathering. The low degree of fracturing of the studied rocks such as quartzite sandstone or organodetrital limestone influences their significant resistance to the investigated geomorphologic process. A. Traczyk and P. Migoń (2000) call attention to differing rates of weathering depending on lithology, petrography and the degree of rock fracturing.

M. Evin (1987) and M. F. André (1996) showed that quartzite rocks are very resistant rocks, which is consistent with observations made for quartzite sandstone. Quartzite sandstone disintegrated the least among the investigated Western Tatra rocks. Nevertheless, A. Martini (1967) labels granite and crystalline limestone as the most resistant rocks.

The studied rock types are more resistant to frost weathering than rocks studied by N. Matsuoka (1990). Comparing measurements of the velocity of the ultrasonic wave, it may be observed that already at the beginning of the laboratory experiment the values of V_p were significantly higher in the case of the rocks in the present study. The initial values ranged from more than 4.0 to more than 6.0 km·s^{-1}, whereas the range was from 1.0 to less than 2.5 km·s^{-1} for the rocks investigated by N. Matsuoka (1990).

Laboratory research results are presented in some publications in terms of mass or a percentage share of weathered material. This manner of presentation of results allows making partial comparisons easy. A. Martini (1967) obtained weathered material in an amount of up to 1% of the initial mass of rock samples, whereas the weathered material generated from the Western Tatra rocks reached 6.8 %. In the case of rocks studied by M. F. André (1993), the maximum amount of weathered material was 9.22% of the initial sample mass. The mass of frost weathering products studied by M. Evin (1987), reached 5.5 g. The rocks in this study produced up to 12.86 g of weathered material (a dolomite sample); however, in most cases the mass of the weathered material did not exceed 1 g.

K. Hall et al. (2002) in their research looked at the big difference in air temperature between the surface and the interior of rocks, noticeable already at a depth of 2 cm. The temperature difference between the interior and the surface layer of a rock results in creating stress within the rock, which is highly significant given the differing degrees of porosity and fissuring of the Tatra rocks.

Z. Rączkowska (2007) stated that primarily large grain-sized material was produced as a result of frost weathering. The measurement of grain size of the weathered material, produced during the simulation of the process in the laboratory, indicated that the weathered material was dominated by the gravel fraction.

D. Draebing and M. Krautblatter (2019) distinguish phases of frost weathering. The rocks contracts during cooling (Phase–1) and expands during warming (Phase–5). Freezing of crack water infill to ice (Phase–2) results in crack opening and ice relaxation due to warming in crack closing (Phase–4). Open systems with water in combination with long-term freezing enables ice segregation-induced crack opening (Phase–3 of ice-segregation tests). The subcritical cracking is the dominant process of frost weathering and progressively decreases the strengths of rockwalls. In nature, can processes may be a factor preparing for a rockfall. Dry and wet cycles (Sass 2005) and rapid temperature changes (Collins and Stock 2016) contribute most.

Based on previous research, it was observed that the significant resistance of the tested Tatra rocks results from low porosity, low water absorption and compactness of the rocks, and good sorting of rock grains. The presence of a binder that almost completely fills the pores of the rock is also important. No influence of texture on the disintegration of rocks was observed, but the presence of mineral veins in the rock determines the manner of their disintegration, visible in the studies of fine-grained conglomerates (Lubera and Krzaklewski 2020).

The studied Western Tatra rocks are characterized by a low susceptibility to frost weathering. It is the least resistant rock is dolomite breccia belongs to the least resistant rocks. The analyses of the physical properties of rocks, which were performed, allowed to identify the properties responsible for high resistance of the studied rocks. The rocks are characterized by low open porosity, which is less than 5% for all types of these rocks. A low degree of fracturing of rock samples in their initial state, infilling of existing pores with a cementing material, primarily in sandstone and conglomerate, and secondary infilling of fractures with cement in limestone rocks, all limit the possibilities of water entering the rocks. The studied Western Tatra rocks are characterized by very low capability to absorb water. Moreover, the physical properties of rocks, which control their high resistance, include their high

strength, especially in sandstone and conglomerate, a large share of quartz rocks in the mineral composition as well as toughness and often mono-mineral rock composition.

The effect of grain orientation within the texture on the resistance of a rock to frost weathering was not observed. However, the presence of carbonate cement and carbonate rock fragments, which were systematically dissolved, within the rock was important, because it created better conditions for physical weathering. In the case of the studied granite and amphibolite rocks, the presence of mica and chlorite in their mineral composition seemed to have a significant influence on the progress of frost weathering. These minerals are the first to get separated from a rock, thus enlarging the voids in that rock. Moreover, the widening of the space between the laminae (sheets) of mica and chlorite occurs as a result of the action of frost weathering.

The issue of filling in rock pores with cement is more complex. If the cement or rock fracture filling is carbonate, made of calcite, then it becomes dissolved over time, and then the action of frost weathering is made easy. This may be observed on the example of fine-grained conglomerate and organodetrital limestone. In the case of clay cement or quartz cement, however, dissolution does not occur. The infilling of rock voids with cement makes it difficult for water to get into the rock, and this way it limits the action of frost weathering. This scenario can be observed on the example of quartzite sandstone.

Observations of the condition of rock samples, performed during the simulation of weathering, have shown how particular rocks disintegrate and how interesting and different this is. Disintegration in carbonate rocks occurs all the time, intensified by the dissolution of rock. Irregular, sharp chips break away and gradually disintegrate further over time. The presence of carbonate fragments or carbonate cement in the mineral composition of rocks plays a crucial role in their disintegration. This influence was apparent on the example of amphibolite and conglomerate samples.

The effect of texture on the disintegration of rocks was not observed, whereas the occurrence of mineral veins in rocks determined the manner in which they disintegrated, as it occurred in samples of fine-grained conglomerate.

It is noteworthy that regardless of the index of resistance to frost weathering used, rock types are arranged in the same order, except granites. Based on the index R_f, Tatra granites are less resistant than indicated by the amount of weathered material produced during the frost weathering simulation.

It seems as though frost weathering of granite rocks is the most interesting issue for research. These rocks, depending on the frost weathering index used, occupy a different place in the presented ranking ordered by resistance of the studied Western Tatra rocks. Measurements of the velocity of the ultrasonic wave allow to draw the conclusion that the rock structure was suffering

damage gradually over an extended period of time, but this was not associated with observable macroscopic changes. It might be expected that a greater number of freeze-thaw cycles would lead to significant disintegration of the rock into a fine-grained, weathered substance. This stands in contrast to quartzite sandstone and amphibolite rocks, in the case of which there was no indication that an acceleration in disintegration had occurred.

Large differences, even within a small part of a rock wall, represent a significant difficulty in the study of rocks and the formulation of broad conclusions. Therefore, the research results presented in this work ought to be understood as referring to particular types of rocks, the physical properties of which have already been characterized in other studies.

REFERENCES

A n d r é M.F., 1993. *Les versants du Spitsberg*. Presses Universitaires de Nancy, Nancy, 131–160.

A n d r é M.F., 1996. *Rock weathering rates in Arctic and Sub-Arctic environments (Abisko Mts., Swedish Lappland)*. Zeitschrift f. Geomorphologie N.F. 40, 4, 499–517.

B a r a n o w s k a J., G a r b i a k M., 1999. *Badania ultradźwiękowe*. Politechnika Szczecińska, Szczecin.

B l a n d W., R o l l s D., 1998. *Weathering: An Introduction to the Scientific Principles*. Oxford. University Press, New York.

C h e n T.C., Y e u n g M.R., M o r i N., 2004. *Effect of water saturation on deterioration of welded tuff due to freeze-thaw action*. Cold Regions Science and Technology 38, 127–136.

C o l l i n s B.D., S t o c k G.M., 2016. *Rockfall triggering by cyclic thermal stressing of exfoliation fractures*. Nature Geoscience 9, 5, 395–400.

C h r z a n T., 1994. *Ultradźwiękowe badania właściwości skał i materiałów budowlanych.* Wyd. Politechnika Wrocławska, Wrocław.

D r a e b i n g D., K r a u t b l a t t e r M., 2019. *The Efficacy of Frost Weathering Processes in Alpine Rockwalls*. Geophysical Reasearch Letters, 46,12, 6516–6524.

E v i n M., 1987. *Lithology and Fracturing control of rock glaciers in southwestern Alp of France and Italy*. [in:] J.R. Giardino, J.F. Shorder, J.D. Vitek (eds.), *Rock Glaciers*. Allen & Unwin, London, 83–160.

G ą d e k B., G r a b i e c M., K ę d z i a S., R ą c z k o w s k a Z., 2016. *Reflection of climate changes in the structure and morphodynamics of talus slopes (Tatra Mountains, Poland)*. Geomorphology 263, 39–49.

H a l l K., 1999. *The role of thermal stress fatigue in the breakdown of rock in cold regions*. Geomorphology 31, 47–63.

H a l l K., T h o r n C., 2010. *The historical legacy of spatial scales in freeze-thaw weathering: Misrepresentation and resulting misdirection*. Geomorphology 130, 83–90.

H a l l K., T h o r n C.E., M a t s u o k a N., P r i c k A., 2002. *Weathering in cold regions: some thoughts and perspectives*. Progress in Physical Geography 26, 4, 577–603.

H a l l e t B., W a l l e t J.S., S t u b b s C.W., 1991. *Weathering by Segregation Ice Growth in Microcracks at Sustained Subzero Temperatures: Verification from an Experimental Study Using Acoustic Emissions*. Permafrost and Periglacial Processes, 2, 283–300

H e s s M., 1965. *Piętra klimatyczne w polskich Karpatach Zachodnich.* Prace Geograficzne UJ 11, 13, 1–237.

L u b e r a E., K r z a k l e w s k i P., 2020. *Wietrzenie mrozowe wybranych skał tatrzańskich w świetle badań laboratoryjnych*. Przegląd Geograficzny 92, 1, 19–39.

Łupikasza E., Szypuła B., 2019. *Vertical climatic belts in the Tatra Mountains in the light of current climate change*. Theoretical and Applied Climatology 136, 249–264.

Martini A., 1967. *Preliminary experimental studies on frost weathering of certain rock types from the West Sudetes*. Biuletyn Peryglacjalny 16, 147–194.

Matsuoka N., 1990. *Mechanisms of rock breakdown by frost action: an experimental approach*. Cold Regions Science and Technology 17, 3, 253–270.

Matsuoka N., 2001. *Microgelivation versus Macrogelivation: Towards Bridging the Gap between Laboratory and Field Frost Weathering*. Permafrost and Periglacial Processes 12, 299–313.

Matsuoka N., Murton J., 2008. *Frost weathering: Recent Advances and Future Directions*. Permafrost and Periglacial Processes 19, 195–210.

Migoń P., 2006. Geomorfologia. PWN, Warszawa.

Nowakowski A., Młynarczuk M., Ratajczak T., Gustkiewicz J., 2003. *Wpływ warunków termicznych na zmianę niektórych właściwości fizycznych i strukturalnych wybranych skał.* Prace Instytutu Mechaniki Górotworu PAN Kraków 5, 29–32.

Paasche Ø., Strømsøe J.R., Dahl S.O., Linge H., 2006. *Weathering characteristics of Arctic islands in northern Norway.* Geomorphology 82, 430–452.

Piotrowska K., Danel W., Iwanow A., Gaździcka E., Rączkowski W., Bezák V., Maglay J., Polák M., Kohút M., Gross P., 2015. *Mapa geologiczna*. [in:] *Atlas Tatr – Przyroda nieożywiona*. Tatrzański Park Narodowy, Zakopane.

Rączkowska Z., 2007. *Współczesna rzeźba peryglacjalna wysokich gór Europy*. Prace Geograficzne IGiPZ PAN 212, 1–252.

Sass O., 2005. *Rock moisture measurements: Techniques, results, and implications for weathering*. Earth Surface Processes and Landforms 30, 3, 359–374.

Traczyk A., Migoń P., 2000. *Cold-climate landform patterns in the Sudetes. Effects of lithology, relief and glacial history*. Acta Universitatis Carolinae 25, Supplementum, 185–210.

Tricart J., 1960. *Prace doświadczalne w zakresie zagadnienia wietrzenia mrozowego*. [in:] J. Tricart (ed.), *Zagadnienia geomorfologiczne*. PWN, Warszawa, 201–234.

Turkington A.V., Paradise R.T., 2005. *Sandstone weathering: a century of research and innovation*. Geomorphology 67, 229–253.

Ewa Lubera, Kazimierz Krzemień, Paweł Krzaklewski
Jagiellonian University
Institute of Geography and Spatial Management
Gronostajowa 7, 30–387 Kraków, Poland
e-mail to corresponding author:pawel.krzaklewski@uj.edu.pl